KenKyu

Kenkyu Journal of Nanotechnology & Nanoscience 6:01-14 (2020)

RESEARCH ISSN: 2455-183X

Effect of Hybridization with rGO/AgNPs on the Photocatalytic Activity of ZnO NPs

Van Manh Nguyen[1*], Xuan Huy Nguyen[1], Tien Viet Vu[1], The Huu Nguyen[1], Tuan Anh Nguyen[2]

[1]Faculty of Chemical Technology, Hanoi University of Industry, BacTu Liem, Hanoi, Vietnam

[2]Institute for Tropical Technology, Vietnam Academy of Science and Technology, Hanoi, Vietnam

Received July 27, 2020**; Accepted** August 14, 2020**; Published** August 15, 2020

***Corresponding author:** Van Manh Nguyen, Faculty of Chemical Technology, Hanoi University of Industry, BacTu Liem, Hanoi, Vietnam; Email: nguyenvanmanh@haui.edu.vn

Abstract

In this study, reduced graphene oxide/ZnO/Ag (rGO/ZnO/Ag) nanohybrids were successfully synthesized. The morphological and optical properties of nanohybrids were characterized by field emission scanning electron microscopy and UV–Vis absorption spectroscopy. The photocatalytic performance in reduction of Cr(VI) to Cr(III) was investigated for both rGO/ZnO/Ag, ZnO/Ag and Ag NPs, with or without UV light irradiation. Photocatalytic study revealed that under UV light irradiation, the rGO/ZnO/Ag nanohybrid exhibited the higher photocatalytic performance in reduction of Cr(VI) to Cr(III), compared to both ZnO and ZnO/Ag nanocatalysts. From this finding, rGO/ZnO/Ag nanohybrid would be the promising nano-photocatalyst for soil and water remediations.

Keywords: ZnO NPs, Ag NPs, rGO, nanohybrids, photocatalysis, hexavalent chromium

1. Introduction

As reported in the literature, metal oxide semiconductor nanoparticles, such as ZnO anh TiO_2, exhibited the phtocatalytic activity under UV light radiation. It refers to the case that a photon having a higher energy than their optical band gap energy (Eg~ 3.2-3.4 ev) is absorbed by these nanoparticles, the electron–hole pairs were created. Since ZnO nanoparticles (ZnO NPs) had a wide band gap (3.37 eV [1]), only UV light (~5% of the solar energy) could be used for the photoactalysis. Besides, ZnO NPs exhibited a low photoenergy conversion efficiency [2] (with low charge separation efficiency and fast recombination of photogenerated charge carriers), which shoud limit their practical uses [3, 4]. Recently, various works have been carried out to improve the photocatalytic of ZnO through two approaches: (i) reduction of the recombination of photogenerated electron–hole pairs, (ii) improvement of the visible light sensitivity (45% of solar energy belongs to visible light). For the first pathway by using the noble metals (Ag), the formation of the Schottky barriers at the interface of noble metals/ZnO NPs, significantly improved the segregation of charges and reduced the charge recombination [5, 6]. On the second pathway, recently, the hybridization of ZnO NPs with

noble metals (Au, Ag, Pd,) defeated strongly the larger band gap of ZnO NPs [7,8]. In this regard, the energy level alignment between the ZnO NPs was combined at the heterojunction. In these nanohybrids, the noble metal nanoparticles (gold and silver) exhibit localized surface Plasmon resonance (LSPR) absorption in visible light which can have significant impact at the heterointerfaces.

Recently, 2D material-supported catalysts have been significantly developped [9] due to their well-defined and precisely located nanocatalytic centers. Among the 2D materials, the reduced graphene oxide (rGO) has been considered as the best promising matrix by having excellent properties (zero band gap, high transmittance, high electron conductivity, larger specific surface area, higher thermal/chemical stability…). As reported in the literature, for the photocatalytic and photoresponsive applications, hybridization with rGO provided many advantages. For exemple, Han et al. [10] found that MoS_2/TiO_2/graphene nanohybrids enhanced light absorption and efficient charge separation properties, by increasing both active adsorption sites and photocatalytic reaction centers. Huang et al. [11] reported that their MoS_2/graphene nanohybrid had the superior photoresponse activities (under sunlight irradiation) in contrast with bare MoS_2 and graphene.The authors indicated that this enhanced photoresponsivity could be attributed to the improved light absorption, strong light–matter interaction and the extremely efficient charge separation.

In case of ZnO-based nano-photocatalysts, by having large specific surface area and fast electron transport [12,13], reduce graphen oxit (rGO) has been considered as promissing materials to transmit effectively the photo-generated electrons of ZnO NPs and then prevent the recombination of photo-generted electron–hole pairs, then improve significantly catalytic efficiency in the rGO/ZnO nanohybrids [14-17].

By a one-step solvothermal method, Yu et al. [18] synthesized Ag–ZnO/rGO nanocomposites .Compared to ZnO, Ag–ZnO and ZnO/RGO nanocatalysts, these Ag–ZnO/RGO nanocomposites exhibitedthe higher photocatalytic performance in degrading methylene blue [22].

As reported, chromium in the hexavalent oxidation state is toxic and carcinogenic. Hexavalent chromium (Cr(VI)) has been found as pollutant in soils, groundwaters, and waste materials. As sodium dichromate, Cr(VI) is used in the chemical industry (producing pigments, wood treatment, tannery products, corrosion inhibitors…). Assadi et al. [19] reported the photocatalytic reduction of Cr(VI) to Cr(III) in aqueous solutions using the ZnO NPs under UV irradiation.

In this study, the hybridization of ZnO NPs and AgNPs/rGO are expected not only to simply combine property of single components, but also to significantly enhance the photocatalytic property of ZnO. Thus, this work aims to present the role of rGO in enhancing the photocatalytic activity of both ZnO NPs and ZnO/Ag nanohybrid.

2. Materials and Methods

2.1 Synthesis of ZnO/Ag nanohybrid

To synthezise the ZnO/Ag, the procedure is below:

- Adding 10,95g $Zn(O_2CCH_3)2(H_2O)$ and 0,255g AgNO3 into an 500 mL Erlenmeyer flask,
- Adding 140mL etylene glycol into the mixture, then magnetically stirring (800 rpm) during 60 minutes at 70 oC.
- Adding gradually 20 mL 0.5 M NaOH, then magnetically stirring during 4 hours at 70^{o}C.
- The ontained mixture is then transferred in to the autoclave (60 oC during 20 hours)
- The obtained mixture is then centrifuged at 4,000 rpm during 30 minutes
- Collecting the precipitation and rinsed by deionized water/etanol

- Final product is then collected and dried at 60˚Cduring 8 hours in air.

2.2. Synthesis of GO

To synthesizethe GO, the procedure(Hummer's method [20]) is below:

- Adding 1g graphite and 0.5g $NaNO_3$ into an 500 mL Erlenmeyer flask,
- Adding 50 mL H_2SO_4 (98%) into the mixture.
- Keeping flask in the ice batch, then magnetically stirring (800 rpm) during 15 minutes.
- Adding gradually 10g $KMnO_4$, then magnetically stirring during 60 minutes
- Magnetically stirring during 60 minutes at 35°C
- Adding 100 mL distilled water into the flask, then magnetically stirring during 30 minutes at 90°C
- Adding gradually 10 mL H_2O_2 (30%) and HCl (0.1M) to remove the residual $KMnO_4$
- The obtained mixture is then centrifuged at 4,000 rpm during 25 minutes
- rGO product is then collected and dried at 60˚C in air.

2.3. Synthesis of ZnO/Ag/rGO nanohybrids

To synthezise the rGO/ZnO/Ag, the procedure is below:

- Adding 10,95g $Zn(O_2CCH_3)_2(H_2O)$, 0,255g $AgNO_3$ and 0,06g GO into an 500 mL Erlenmeyer flask,
- Adding 140mL etylene glycol into the mixture, then magnetically stirring (800 rpm) during 60 minutes at 70°C.
- Adding gradually 20 mL 0.5 M NaOH , then magnetically stirring during 4 hours at 70 oC.
- The ontained mixture is then transferred in to the autoclave (60°C during 20 hours)
- The obtained mixture is then centrifuged at 4,000 rpm during 30 minutes
- Collecting the precipitation and rinsed by deionized water/etanol
- Final product is then collected and dried at 60˚C during 8 hours in air.

2.4. Characterization

FESEM and EDX Chracterization Field Emission Scanning Electron Microscopy S 4800 (Hitachi, Japan). The coating surface was coated with a very thin carbon layer to avoid the charging effect caused by nonconductive nature of coatings.

UV–Vis spectra were obtained using a LAMBDA™ 35 spectrophotometer (PerkinElmer, Waltham, MA, USA) in absorbance mode.

2.5. Photocatalytic activity evaluation

2.5.1. Photocatalytic reduction of Cr(VI) to Cr(III) test

For the test of photocatalytic reduction of Cr(VI) to Cr(III), the procedure is below:

- Adding 0,1g nanomaterials into 100mL Crom(VI) solution ($K_2Cr_2O_7$), with the known concentration and pH.
- The mixture then covered and kept in dark, then magnetically stirring (500 rpm) during 30 minutes for the reaction before UV irradiation
- The mixture then moved to the UV chamber (UVA-340 / 15W : 4 Lamps), during 140 minutes, under magnetically stirring (6,000 rpm).
- -The obtained mixture is then centrifuged, removed the precipitation, before the solution was subjected to UV-vis spectroscopy.

2.4.2. Quantifying Cr6+ concentration in solution

The ultraviolet (UV)-visible absorbance spectroscopy is a proven techique for accurately detecting hexavalent chromium in aqueous solutions [21, 22]. In this work, Spectroscopy LAMBDA 35 (USA) was used for hexavalent chromium quantification.

Potassium dichromate ($K_2Cr_2O_7$ analytical grade, Sigma Aldrich) was used to prepare a Cr(VI) stock solution of 1 g/L. Vissibly, the color of an aqueous Cr(VI) solution is yellow. Standard solutions were made by diluting aliquots of this stock solution with deionized water.By testing 7 standard Cr(VI) aqueous solutions of $K_2Cr_2O_7$ (10 mg/L to 70 mg/L, pH =7), a calibration curve was established to correlate theoptical density at the characteristic peaksand the Cr6+ concentration.

As seen in this Figure 1, there are two absorbance wavelengths of Cr(VI) absorptionlays at 260 nm and 373 nm. At 260 nm peak of charge transfer transition between O and Cr(VI) is observed [23].

However this absorption bandis generally not used for Cr(VI) quantification [21]. Then the absorption wavelength of 373 nm is generally used in other published works [23-27].

In this study, we use the charateristic band at 373 nm for quantifying Cr(VI) concentration in solution. The calibration curve was then used to determine the Cr(VI) concentration after treatments (at λ =373 nm, Figure 1).As shown in Figure2, the calibration curves established with these standard solutions of Cr(VI) showed a strong linear correlation between the Cr(VI) concentration and optical density (with a very high R-square value of 0.999).

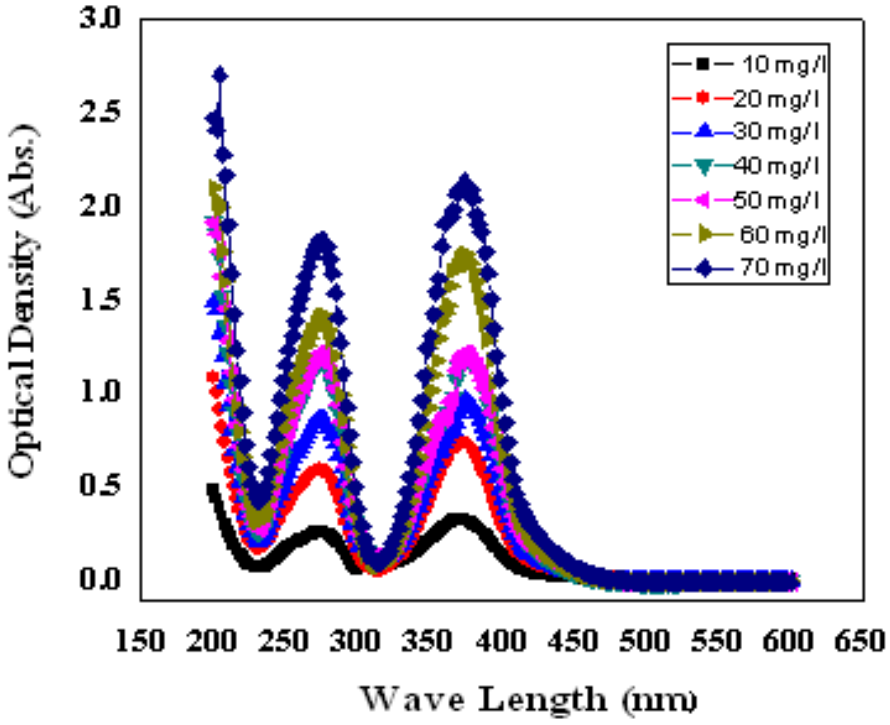

Figure 1: UV-visible spectra of7 standard Cr(VI) aqueous solutions at pH =7

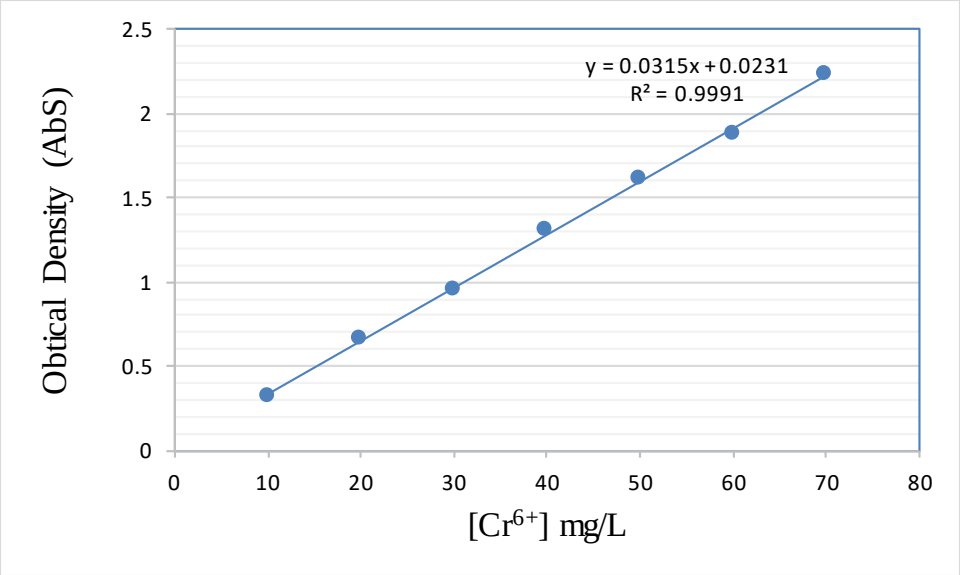

Figure 2: Calibration curve in Cr (VI) aqueous solutions at λ = 373 nm.

The efficiency in reduction of Cr(IV) can be calculated by following equation:

$$\text{Efficiency (H)}\ \% = \frac{A_o - A_i}{A_o} = \frac{C_o - C_i}{C_o} \times 100\%$$

Where:

A_0: Optical density for the initial solution (before treatment)

A_i: Optical density for the final solution (after treatment)

C_0: Initial Cr(VI) concentration (mg/L)

C_i : Final Cr(VI) concentration (mg/L)

3. Results and Discussions

3.1. Characterization of ZnO NPs, ZnO/Ag and rGO/ZnO/Ag nanohybrids

Figures 3-5 show the electron microscopy images of ZnO NPs, ZnO/Ag nanohybrid and rGO/ZnO/Ag nanohybrids, respectively. As seen in Figure 3, SEM images showed the ZnO hexagonal rods (~100-150 nm). Whereas, in Figure 4 as compared to Figure 3, the avarage size of ZnO/Ag nanohybrid is higher than that of ZnO NPs. A possible explanation is that AgNPs might act as the nucleus for formation/synthesis of ZnO during hybridization.

Figure 6 presents the EDX measurement for rGO/ZnO/Ag nanohybrid. EDX data confirmed the presence of AgNPs in the nanohybrids. Combination Figures 5 and 6 indicated that ZnO/Ag nanohybrids was dispersed into rGO matrix.

To verify the hybridization of ZnONP and AgNPs, UV-vis spectra are collected for the aqueous solutions containing ZnO NPs and ZnO/Ag nanohybrids. Figure 7 presents the UV-visible spectra of ZnO NP and Ag/ZnO nanohybrids dispersed in water. As can be seen in Figure 7, the absorption band for pure ZnO is observed in the UV region (at ~270 nm), whereas

it was shifted to the visible region for Ag/ZnO nanohybrids due to the contribution of the AgNPs localized surface Plasmon resonance (LSPR) absorption at 375 nm. Please note that the average size of ZnO NPs is slightly smaller than that of Ag/ZnO nanohybrids (by this method for their synthesis) as shown in Figures 3 and 4.

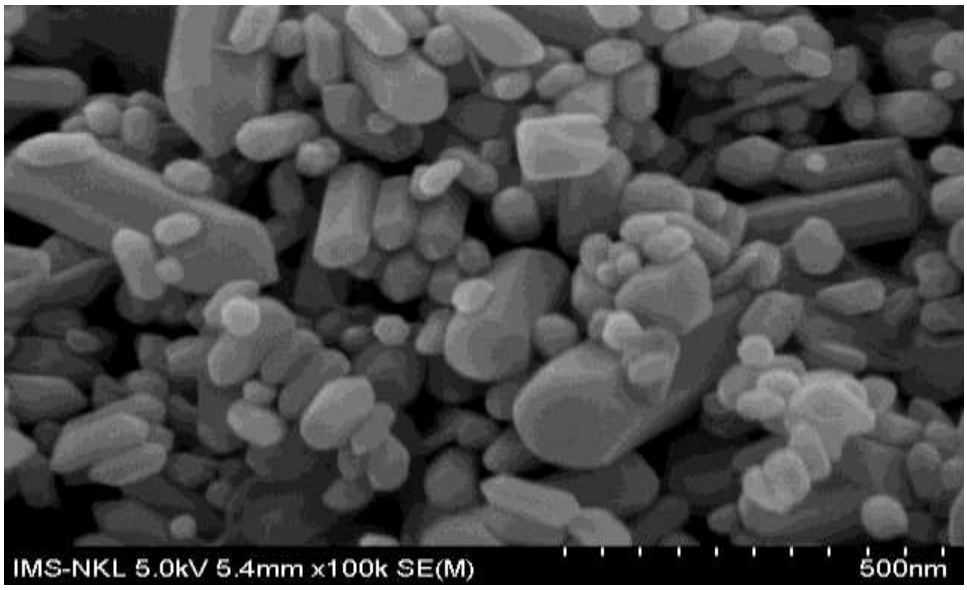

(a)

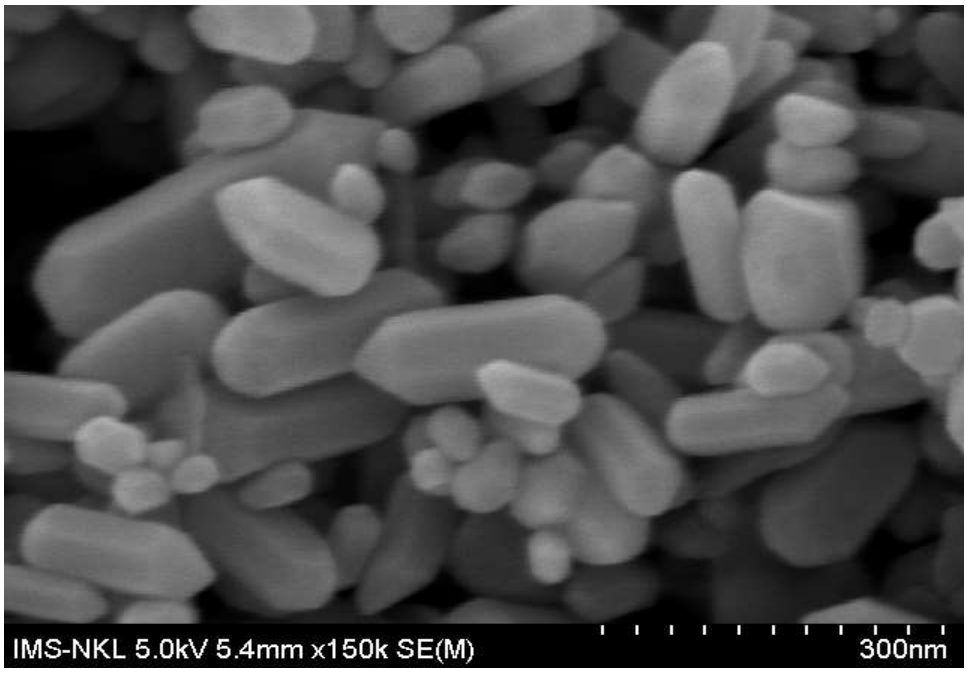

(b)

Figure 3: FE-SEM image of ZnO nanoparticles. Magnification: a) × 100,000; b) × 150,000

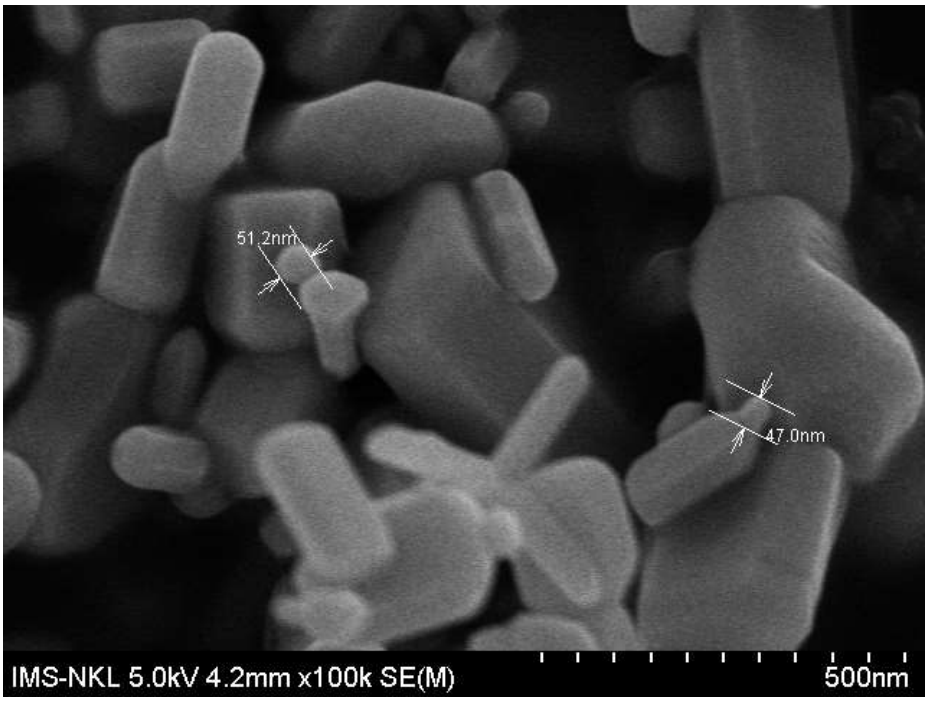

(a)

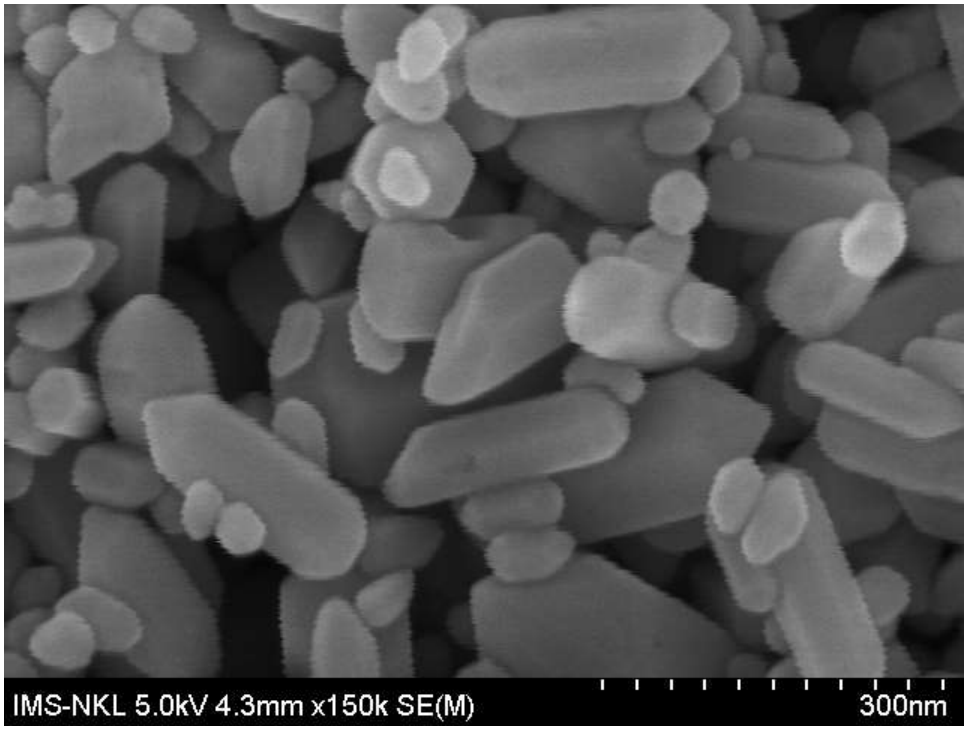

(b)

Figure 4: FE-SEM image of ZnO/Ag nanohybrids. Magnification: a) × 100,000; b) × 150,000

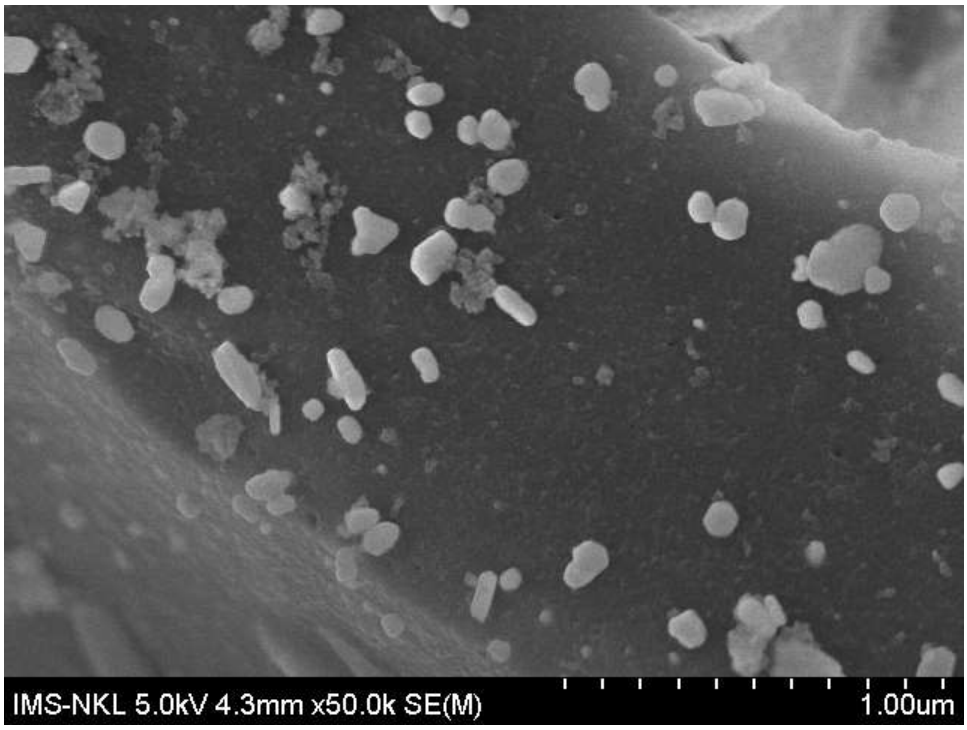

(a)

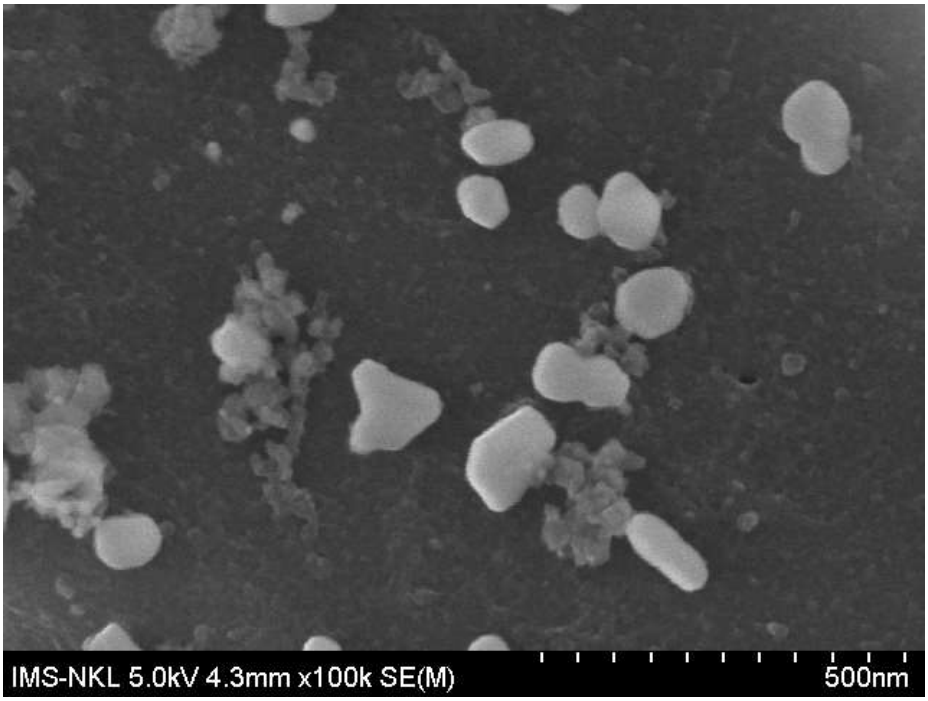

(b)

Figure 5: FE-SEM image of rGO/ZnO/Ag nanohybrids. Magnification: a) × 50,000 b) × 100,000

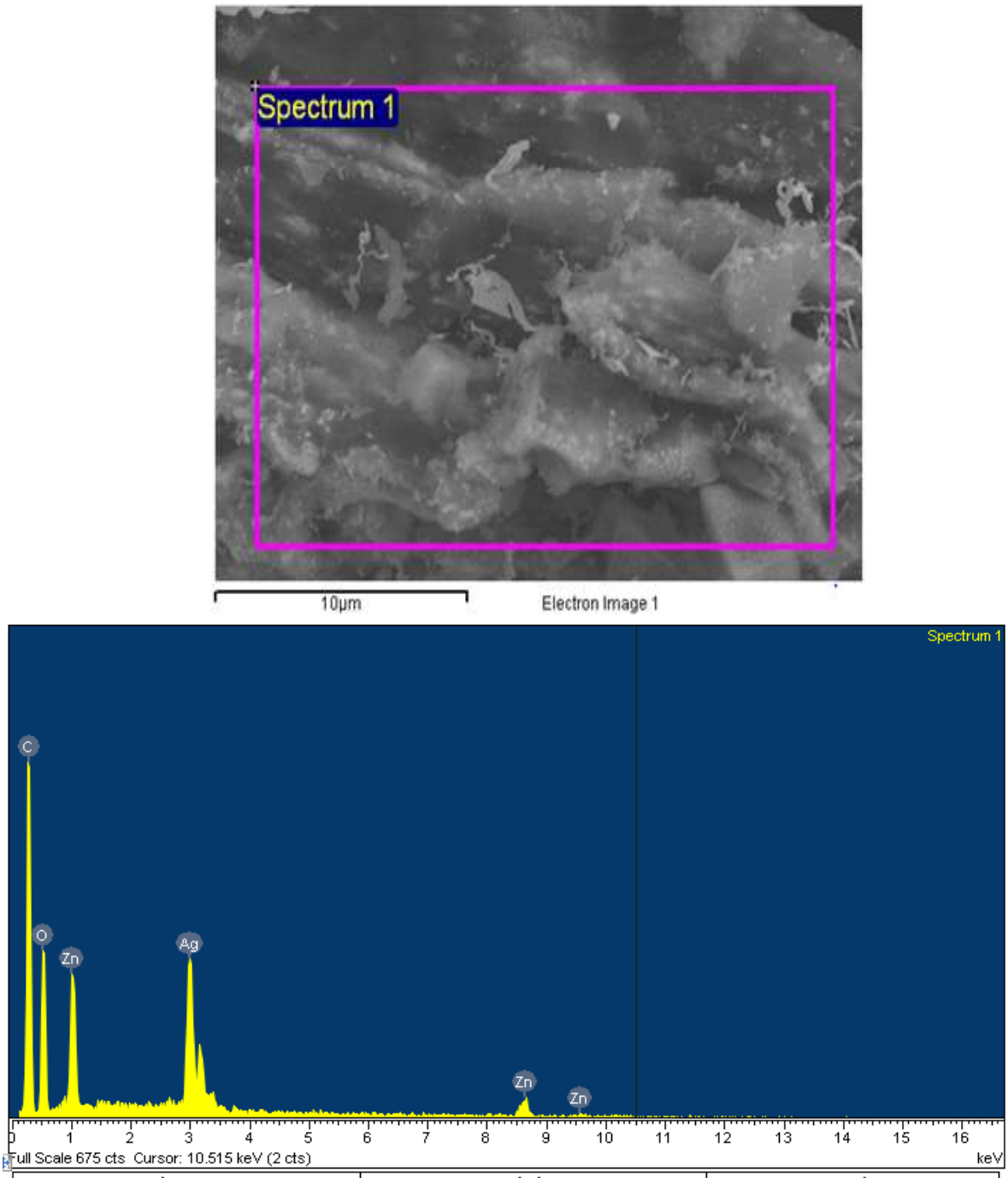

Element	Weight %	Atomic %
C K	39,68	55,79
O K	38,08	40,20
Zn K	5,24	1,35
Ag L	17,00	2,66
Totals	100,00	

Figure 6: EDX result of rGO/ZnO-Ag nanohybrid (sample area: 15×20 µm)

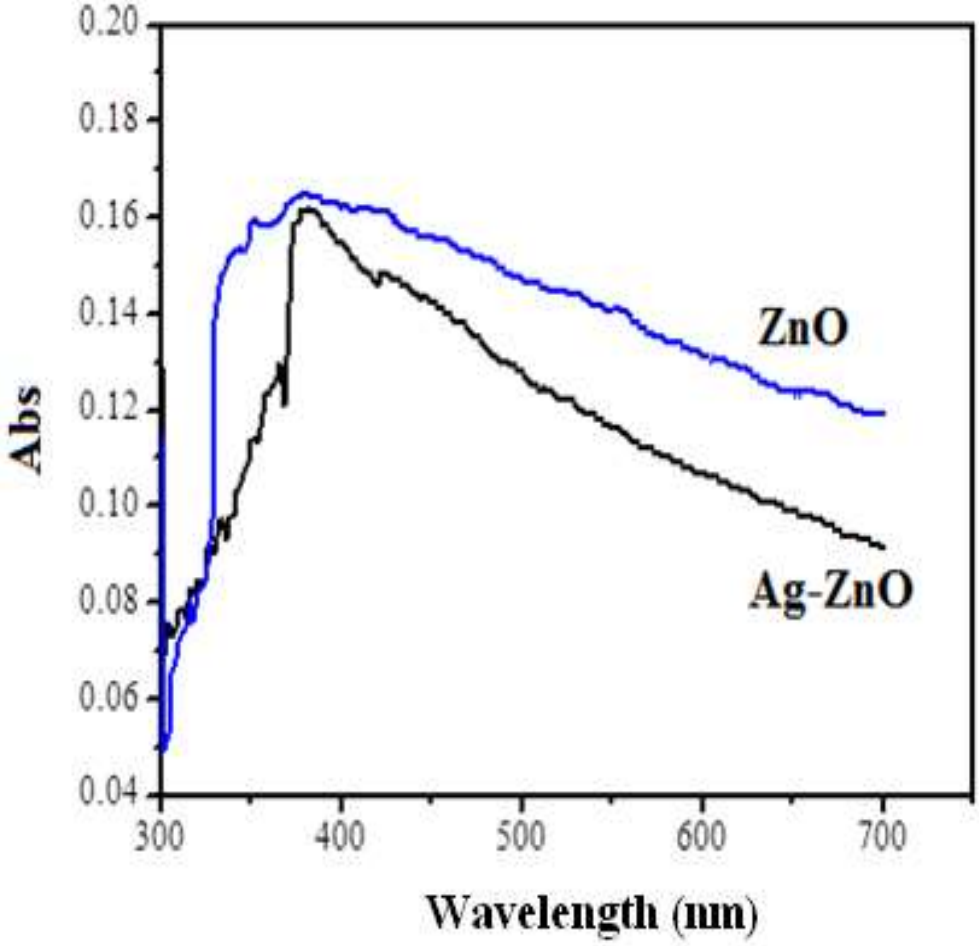

Figure 7: UV-visible spectra of ZnO NP and Ag/ZnO nanohybrids dispersed in water

3.2. Photocatalytic evaluation

3.2.1. Effect of GO and AgNPs on the photocatalytic efficiency of ZnO NPs

Figure 8 presents the values of efficiency for photocatalytic reduction of Cr(VI) to Cr(III) when used ZnO, ZnO/Ag and rGO/ZnO/Ag as nanocatalysts, with or without UV light irradiation.

In case of without UV light irradiation, the efficiency in reduction of Cr(IV) is very low (<3%), with ZnO/Ag NPs nanohybrid being the highest. These low values of efficiency could be attributed to the absorption of Cr(IV) on the surface of nanomaterials in the solution. In addition, since these 3 samples exposed only in room light (during 20 minutes), this result also indicates that hybridization with AgNPs could enhance slightly the light sensitivity in the visible light region of ZnO [28].

In case of UV light irradiation, the efficiency in reduction of Cr(IV) increased strongly (upto 70%), with ZnO/Ag NPs nanohybrid being the highest. As seen in Figure 7, hybridization with AgNPs increased the efficiency of ZnO NPs from 8.2 % to 56.6%. Whereas, hybridization with rGO increased the efficiency of ZnO/Ag nanohybrid from 56.6 % to 69.8%.

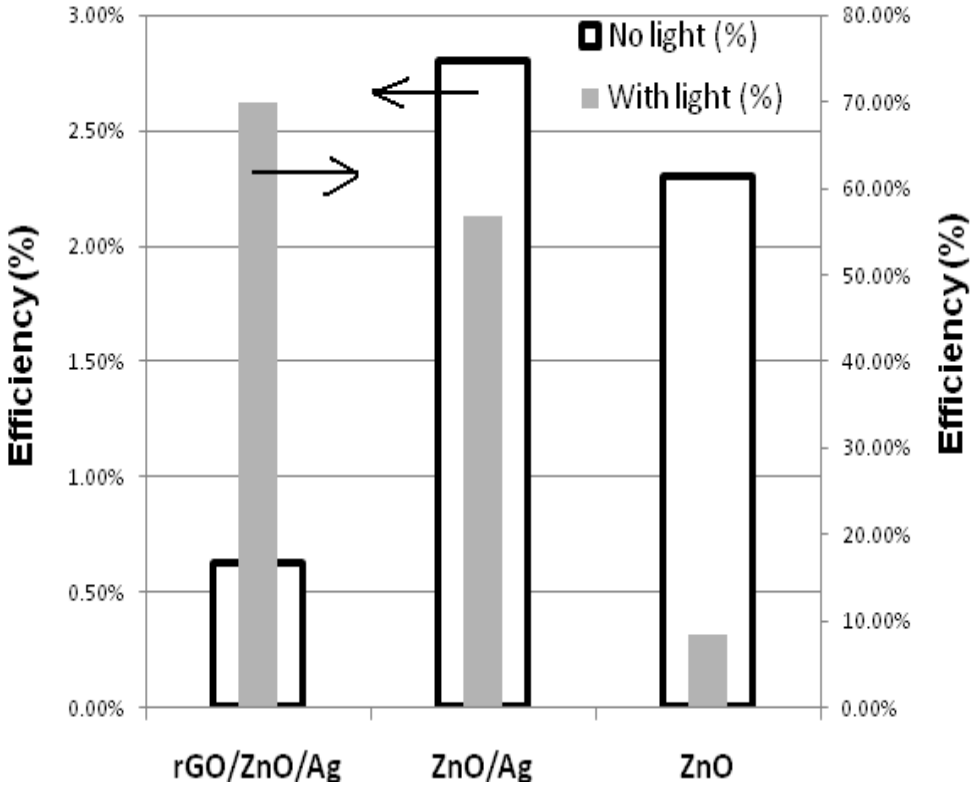

Figure 8: Values of efficiency for photocatalytic reduction of Cr(VI) to Cr(III) when used ZnO, ZnO/Ag and rGO/ZnO/Ag as nanocatalysts, with or without UV light irradiation. (Initial Cr(VI): 50 mg/L at pH 7)

3.2.2. Effect of pH on the photocatalytic efficiency of rGO/ZnO/Ag nanohybrid

Since the main component of catalytic materials are ZnO NPs, the rGO/ZnO/Ag nanohybrid is stable only in neutral aqueous solutions (at pH 7). However, as reported in the literature, the Cr(VI) exhibited the different bands for charge transfer absorption in acid and alkaline solutions [29-31]. Thus, in this study, we try to evaluate the effect of pH on the photocatalytic efficiency of rGO/ZnO/Ag nanohybrid.

Figure 9 presents the values the efficiency for photocatalytic reduction of Cr(VI) to Cr(III) when used rGO/ZnO/Ag as nanocatalysts in different pH values, with or without UV light irradiation. As expected, under light irradiation the efficiency for photocatalytic reduction of Cr(VI) to Cr(III) is higher than without light irradiation, in all 3 solutions of different pH values.

As shown in Figure 9, pH 7 provided a higher efficiency for photocatalytic reduction of Cr(VI) to Cr(III). In pH 10, the newly formed product of , $Cr(OH)_3$ could deposite on the surface of nanocatalysts, thus inhibited their photocatalysis. In case of pH 5, Sanchez-Hachair and Hofmann [21] found the shift in the absorption band from 373nm to 350 nm is due to the hydrogen bond responsible for breakage of a double covalent bond between oxygen and the Cr ion. The authors inferred that the photon energy transfer is higher when Cr(VI) species have two double bonds (photon energy transfer in pH 5 would be lower than that of pH 7 and pH 10).

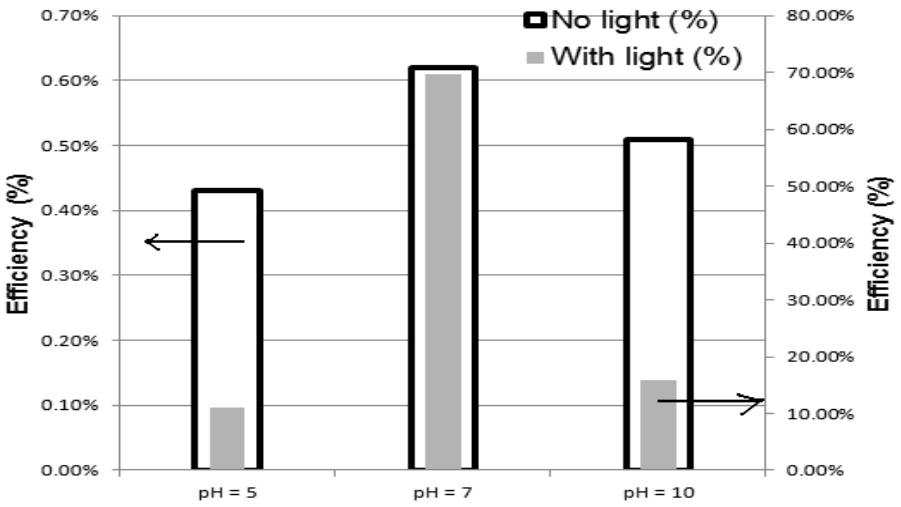

Figure 9: Effect of pH on the efficiency for photocatalytic reduction of Cr(VI) to Cr(III) for rGO/ZnO/Ag as nanocatalysts, with or without UV light irradiation. (Initial Cr(VI): 50 mg/L)

3.2.3. Effect of Cr(VI) concentration on the photocatalytic efficiency of rGO/ZnO/Ag nanohybrid

Figure 10 presents the values the efficiency for photocatalytic reduction of Cr(VI) to Cr(III) when used rGO/ZnO/Ag as nanocatalysts in different Cr(VI) initial concentrations (such as 25, 35 and 50 mg/L in the neutral aqueous solution of pH 7).

As can be seen in Figure 10, the lower Cr(VI) concentration (25 mg/L) has a higher efficiency for photocatalytic reduction of Cr(VI) to Cr(III), upto 90% under UV light irradiation. One possible reason is the dispersibility of nanocatalyst in Cr(VI) aqueous solutions.

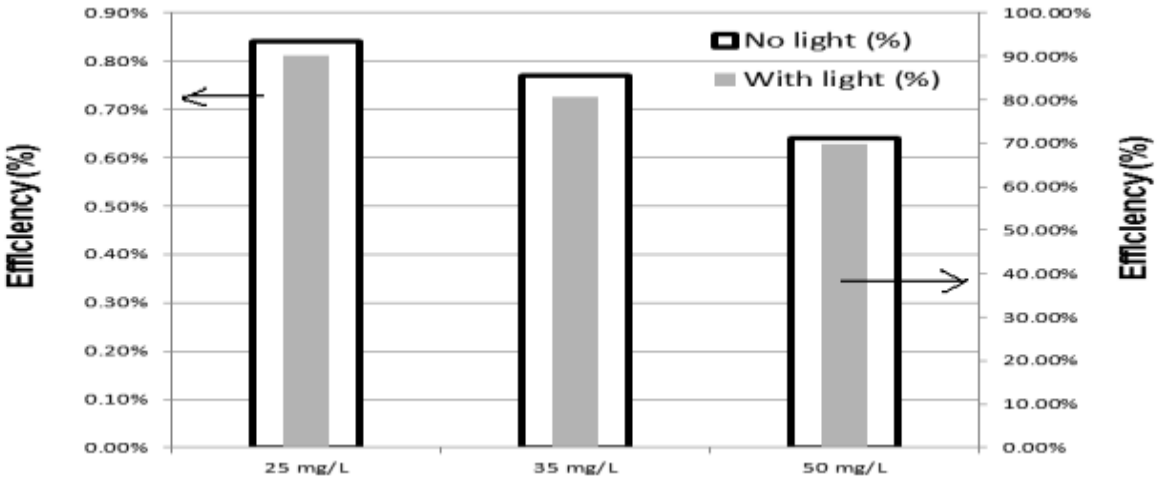

Figure 10: Effect of initial Cr(VI) concentration on the efficiency for photocatalytic reduction of Cr(VI) to Cr(III) for rGO/ZnO/Ag as nanocatalysts, with or without UV light irradiation. (pH =7)

4. Conclusions

The main findings of this study are:

- rGO/ZnO/Ag nanohybrid was successfully synthesized
- Under UV light irradiation, the rGO/ZnO/Ag nanohybrid exhibited the higher photocatalytic performance in reduction of Cr(VI) to Cr(III), compared to both ZnO and ZnO/Ag nanocatalysts.
- As compared to the Cr (VI) solution at pH 5 and pH 10, the pH 7 solution provided a higher efficiency for photocatalytic reduction of Cr(VI) to Cr(III), upto 70% with 50 mg/L of Cr(VI).
- The lower Cr(VI) concentration (25 mg/L) has a higher efficiency for photocatalytic reduction of Cr(VI) to Cr(III), upto 90% under UV light irradiation.
- rGO/ZnO/Ag nanohybrid would be the promising nano-photocatalyst for soil and water remediations.

Acknowledgments: This work was financially supported by Hanoi University of Industry in Vietnam

References

1. H. Gholap, S. Warule, J. Sangshetti, G. Kulkarni, A. Banpurkar, S. Satpute, R. Patil, Hierarchical nanostructures of Au@ZnO: antibacterial and antibiofilm agent, Appl Microbiol Biotechnol, 100 (13) (2016) 5849-5858. doi: 10.1007/s00253-016-7391-1
2. Y Tamaki, K Hara, R Katoh, M Tachiya, A Furub Femtosecond visible-to-IR spectroscopy of TiO2 nanocrystalline films: elucidation of the electron mobility before deep trapping. J Phys Chem C, 113 (2009) 11741–11746
3. X. Chen, S.S. Mao, Titanium dioxide nanomaterials: synthesis, properties, modifications and applications, Chem. Rev. 107 (2007) 2891-2959.
4. A.Kudo, Y. Miseki, Heterogeneous photocatalyst materials for water splitting, Chem. Soc. Rev. 38 (2009) 253-278
5. L. Sun, J. Li, C. Wang, S. Li, Y. Lai, H. Chen, C. Lin, Ultrasound aided photochemical synthesis of Ag loaded TiO2 nanotube arrays to enhance photocatalytic activity, J. Hazard. Mater. 171 (2009) 1045-1050.
6. Md. A. A. Mamun, Y. Kusumoto, T. Zannat, S. Md Islam, Synergistic enhanced photocatalytic and photothermal activity of Au@TiO2 nanopellets against human epithelial carcinoma cells, Phys. Chem. Chem. Phys. 13 (2011) 21026-21034.
7. S. Sakthivel, M.V. Shankar, M. Palanichamy, B. Arabindoo, D.W. Bahnemann, V.Murugesan, Enhancement of photocatalytic activity by metal deposition:characterisation and photonic efficiency of Pt, Au and Pd deposited on TiO2 catalyst, Water Res. 38 (2004) 3001–3008.
8. N. V. Long, N. D. Chien, T. Hayakawa, H. Hirata, G. Lakshminarayana, M. Nogami, The synthesis and characterization of platinum nanoparticles: a method of controlling the size and morphology, Nanotechnology, 21 (2010) 035605, doi:10.1088/0957-4484/21/3/035605
9. Bin Zhang, Taojian Fan, Ni Xie, Guohui Nie, Han Zhang, Versatile Applications of Metal Single-Atom@ 2D Material Nanoplatforms, Advanced Science 6 (21), 1901787, 2019
10. Weijia Han, Chen Zang, Zongyu Huang, Han Zhang, Long Ren, Xiang Qi, Jianxin Zhong, Enhanced photocatalytic activities of three-dimensional graphene-based aerogel embedding TiO2 nanoparticles and loading MoS2 nanosheets as Co-catalyst, International journal of hydrogen energy 39 (34), 19502-19512, 2014
11. Zongyu Huang, Weijia Han, Hongli Tang, Long Ren, D Sathish Chander, Xiang Qi and Han Zhang, Photoelectrochemical-type sunlight photodetector based on MoS2/graphene heterostructure, 2015 2D Mater. 2 (3) 035011. DOI: https://doi.org/10.1088/2053-1583/2/3/035011
12. Ravi Kant Upadhyay, et al., Role of graphene/metal oxide composites as photocatalysts, adsorbents and disinfectants

in water treatment: a review, RSC Adv., 4,3823–3851 (2014)

13. Sung Hong Hahn, et al.,Fast and effective electron transport in a Au–graphene–ZnO hybrid for enhanced photocurrent and photocatalysis, RSC Adv., 5, 63964-63969 (2015)
14. B.J. Li, H.Q. Cao, J. Mater. Chem. 21, 3346–3349 (2011)
15. T. Xu, L. Zhang, H. Cheng, Y. Zhu, Appl. Catal. B 101, 382–387 (2011)
16. M. Ahmad, E. Ahmed, Z.L. Hong, J.F. Xu, Appl. Surf. Sci. 274,273–281 (2013)
17. B. Li, T. Liu, Y. Wang, Z. Wang, J. Colloid Interface Sci. 377,114–121 (2012)
18. Xiaochen Yu, Zhe Li, Kuaile Dang, Zhaoguang Zhang, Lin Gao, Li Duan, Ziqiang Jiang, Jibin Fan, Peng Zhao. Enhanced photocatalytic activity of Ag–ZnO/RGO nanocomposites for removal of methylene blue. Journal of Materials Science: Materials in Electronics, May 2018, Volume 29, Issue 10, pp 8729–8737
19. Anvar Assadi, Mohammad Hadi Dehghani, Noushin Rastkri, Simin Nasseri, Amir Hossein Mahvi, Photocatalytic Reduction of Hexavalent Chromium In Aqueous Solutions With Zinc Oxide Nanoparticles And Hydrogen Peroxide, Environment Protection Engineering, 2012, Vol. 38, No. 4.
20. W.S. Hummers Jr, R.E. Offeman, J. Am. Chem. Soc. 80, 1339–1339 (1958)
21. Arnaud Sanchez-Hachair and Annette Hofmann, Hexavalent chromium quantification in solution: Comparing direct UV–visible spectrometry with 1,5-diphenylcarbazide colorimetry, Comptes Rendus Chimie, Volume 21, Issue 9, September 2018, Pages 890-896. https://doi.org/10.1016/j.crci.2018.05.002
22. Marie–Christine Fournier–Salaun, Philippe Salaun, Quantitative determination of hexavalent chromium in aqueous solutions by UV-Vis spectrophotometer, Central European Journal of Chemistry 5(4) 2007 1084–1093. DOI: 10.2478/s11532-007-0038-4
23. A.Bensalem, B.M. Weckhuysen, R.A. Schoonheydt, J. Phys. Chem. B 101 (1997) 2824-2829.
24. I.J. Buerge, S.J. Hug, Environ. Sci. Technol. 32 (1998) 2092-2099.
25. I.J. Buerge, S.J. Hug, Environ. Sci. Technol. 31 (1997) 1426-1432.
26. S.J. Hug, H.-U. Laubscher, B.R. James, Environ. Sci. Technol. 31 (1997) 160-170.
27. D. Kim, J. Om, Univers. J. Eng. Sci. 1 (2013) 1-4.
28. Van Thang Nguyen, Viet Tien Vu, The Huu Nguyen, Tuan Anh Nguyen, Van Khanh Tran and Phuong Nguyen-Tri, Antibacterial Activity of TiO2- and ZnO-Decorated with Silver Nanoparticles, Journal of composites science, 2019, 3(2), 61; https://doi.org/10.3390/jcs3020061
29. I.J. Buerge, S.J. Hug, Environ. Sci. Technol. 32 (1998) 2092-2099.
30. I.J. Buerge, S.J. Hug, Environ. Sci. Technol. 31 (1997) 1426-1432.
31. S.J. Hug, H.-U. Laubscher, B.R. James, Environ. Sci. Technol. 31 (1997) 160-170.